Wiley
European Journal of Cancer Care
Volume 2025, Article ID 8427059, 16 pages
https://doi.org/10.1155/ecc/8427059

WILEY

Research Article

Cancer-Derived Exosomal miR-146a Promotes Angiogenesis by Suppressing TIMP3 in Colorectal Cancer

He Liu,[1] **Tianyi Xia**,[2] **Song Xiang**,[1] **Zhenzhou Chen**,[1] **Yang Pan**,[1] **Xiaolong Liang**,[1] **and Zhengqiang Wei**[1]

[1]*Department of Gastrointestinal Surgery, The First Affiliated Hospital of Chongqing Medical University, Chongqing, China*
[2]*Department of Colorectal Surgery, Harbin Medical University Cancer Hospital, Harbin Medical University, Harbin 150000, Heilongjiang Province, China*

Correspondence should be addressed to Xiaolong Liang; 202293@hospital.cqmu.edu.cn and Zhengqiang Wei; 205067@hospital.cqmu.edu.cn

Received 31 March 2025; Revised 14 October 2025; Accepted 17 November 2025

Academic Editor: Tao Yu

Background: Tumor progression and recurrence are major contributors to the poor prognosis of colorectal cancer (CRC), with angiogenesis playing a critical role in these processes. Although tumor-derived exosomes are hypothesized to significantly promote angiogenesis, the underlying mechanisms in CRC remain poorly understood.
Methods: Serum exosomal samples from five paired CRC and non-CRC patients were sequenced to identify differentially expressed miRNAs. The biological function of miR-146a and its downstream targets in angiogenesis were investigated using in vitro and in vivo models.
Results: Our findings demonstrate that miR-146a is highly enriched in CRC-derived exosomes, and its expression in serum exosomes is significantly elevated in CRC patients compared to healthy controls. MiR-146a can be transferred from CRC cells to human umbilical vein endothelial cells (HUVECs) via exosomes, enhancing their proliferation, migration, and tube formation. Mechanistically, exosomal miR-146a promotes these proangiogenic effects by downregulating the tissue inhibitor of metalloproteinase 3 (TIMP3) in HUVECs. Furthermore, in vivo experiments confirmed that exosomal miR-146a from CRC cells drives tumor growth and angiogenesis.
Conclusions: This study highlights exosomal miR-146a as a key driver of angiogenesis in CRC, suggesting its potential as a therapeutic target for antiangiogenic strategies in CRC treatment.

Keywords: angiogenesis; colorectal cancer; exosomes; miR-146a; TIMP3

1. Background

Colorectal cancer (CRC) ranks as the third leading cause of cancer-related mortality worldwide, primarily due to its high rates of recurrence and metastasis [1–3]. A hallmark of CRC is its ability to induce angiogenesis [4–6]. The formation of tumor-associated vasculature plays a pivotal role in supplying nutrients to support tumor growth and is critically involved in various aspects of tumor biology, including metastasis, metabolic dysregulation, and the maintenance of cancer stem cells [7–10]. Therefore, elucidating the precise molecular mechanisms underlying angiogenesis is essential for developing effective therapeutic strategies against CRC.

Micro-RNAs (miRNAs) are a class of small noncoding RNAs that function as post-transcriptional regulators of gene expression by binding to target mRNAs and suppressing their translation [11–15]. Emerging evidence has demonstrated that miRNAs play a pivotal role in modulating endothelial cell (EC) function during tumor angiogenesis [16–18]. Specifically, miRNAs derived from tumor cells can regulate the expression of proangiogenic or antiangiogenic factors, thereby influencing EC proliferation, migration, and

tube formation [19–21]. Notably, miRNAs can be encapsulated within exosomes, which are extracellular vesicles approximately 100 nm in diameter [22]. Exosomes are secreted by various cell types into the circulation and can transport their cargo, including miRNAs, to recipient cells across the body [23]. Through this mechanism, exosomes exert regulatory effects on target cells, including the modulation of gene expression [24–26]. Of particular relevance, tumor-derived exosomes have been shown to deliver miRNAs to ECs, thereby promoting angiogenesis [27]. Furthermore, exosomes have been implicated in enhancing CRC progression by facilitating angiogenesis. These findings suggest that targeting exosomal miRNAs may represent a promising therapeutic strategy to inhibit tumor angiogenesis [28].

In this study, we first identified miR-146a as a highly abundant miRNA in the serum of CRC patients and in exosomes secreted by CRC cells. We further demonstrated that CRC-derived exosomal miR-146a can be transferred to human umbilical vein endothelial cells (HUVECs), where it promotes angiogenesis by downregulating the expression of the tissue inhibitor of metalloproteinase 3 (TIMP3). Additionally, using a mouse tumor xenograft model, we confirmed that miR-146a significantly enhances CRC growth and angiogenesis in vivo. Collectively, our findings highlight the critical role of exosomal miR-146a in driving angiogenesis and suggest that targeting this miRNA may offer a novel therapeutic avenue for the treatment of CRC.

2. Materials and Methods

2.1. Human Tissue Acquisition and Ethical Approval. This study was conducted in accordance with the ethical guidelines and approved by the Ethics Committee of Harbin Medical University Cancer Hospital. Written informed consent was obtained from all participants, including patients and healthy donors. Patients with primary CRC underwent curative surgical resection, and none had received preoperative treatments such as chemotherapy or radiotherapy. Serum samples were collected preoperatively and 1 week postoperatively to assess changes in the exosomal content. For RNA sequencing, serum exosomes were isolated from 10 patients, comprising five with metastatic CRC (mCRC) and five with nonmetastatic CRC (non-mCRC). Sequencing was performed by Novogene (Beijing, China). Additionally, fresh CRC biopsy specimens and adjacent normal mucosa were obtained from Peking University Shenzhen Hospital (2020-322). Tissue samples were immediately snap-frozen in liquid nitrogen and stored at −80°C for subsequent analysis.

2.2. Cell Culture. HUVECs, the human colon epithelial cell line NCM460, and CRC cell lines (HCT116, SW480, SNU-C1, and Lovo) were maintained in the Myocardial Ischemia Laboratory at Harbin Medical University. NCM460, HCT116, SW480, SNU-C1, and Lovo cells were cultured in the RPMI-1640 medium supplemented with 10% fetal bovine serum (FBS; ExCell Bio, FSP500, South America). HUVECs were grown in the EC medium (ECM, Cat. No. 1001) containing 10% FBS (ExCell Bio, FSP500, South America). All cells were maintained under standard culture conditions (37°C, 5% CO_2).

2.3. Exosome Isolation and Characterization. Exosomes were isolated from the conditioned media of CRC cells and serum samples from both human and mouse sources. Cells were cultured in a medium supplemented with 10% exosome-depleted FBS (C38010050, VivaCell, Shanghai, China) to minimize contamination. Briefly, cell supernatants (collected after 48 h) or serum samples were subjected to sequential centrifugation at 300 × g and 3000 × g for 10 min each to remove cellular debris. The clarified supernatants were then filtered through a 0.22-μm membrane and ultracentrifuged at 120,000 × g at 4°C for 1 h. The resulting exosome pellets were resuspended in phosphate-buffered saline (PBS), and the exosome concentration was quantified using a BCA protein assay kit (Keygen Biotech). Exosome size distribution and concentration were further analyzed using nanoparticle tracking analysis (NTA) with a Nanosight instrument (version 2.3). For this, exosomes were irradiated with a laser, and their Brownian motion was recorded over a 10-s video.

2.4. Transmission Electron Microscopy (TEM). The morphology of isolated exosomes was examined by TEM (H-7650, Hitachi, Japan). Briefly, 10 μL of freshly prepared exosome suspension was placed onto a carbon-coated copper grid and allowed to adsorb for 10 min at room temperature. Excess liquid was gently removed with filter paper, followed by negative staining with 2% phosphotungstic acid (pH 7.0) for 1 min. The grids were then air-dried at room temperature and visualized under TEM at an accelerating voltage of 80 kV. Images were captured digitally, and exosome morphology was confirmed by their typical cup-shaped appearance with diameters of approximately 100–150 nm.

2.5. Exosome Labeling and Cellular Uptake Assay. Exosomes were labeled with the fluorescent membrane dye PKH67 (Sigma) to track their uptake by recipient cells. Labeled exosomes were incubated with HUVECs for 3 h, after which cells were fixed and counterstained with Hoechst to visualize nuclei. Cellular internalization of exosomes was assessed by fluorescence microscopy (JEM-1220, JEOL, Japan). For functional assays, 1×10^5 HUVECs were cocultured with 50 μg of exosomes to evaluate their effects on EC behavior.

2.6. RNA Isolation and Quantitative Real-Time PCR (qRT-PCR). Total RNA was isolated using the miRcute miRNA Isolation Kit (Tiangen Biotech, China), following the manufacturer's instructions. Subsequently, RNA was reverse-transcribed into complementary DNA (cDNA) using the miRcute Plus miRNA First-Strand cDNA Synthesis Kit (Tiangen Biotech, China). A qRT-PCR was performed on

a 7500 Fast Real-Time PCR System (Applied Biosystems, USA) to quantify gene expression. The relative expression levels of miR-146a were normalized to the endogenous control U6, while TIMP3 mRNA expression was normalized to GAPDH. For exosomal miRNA quantification, cel-miR-39 (Applied Biosystems, CA, USA) was used as an external control to account for variations in the RNA extraction efficiency. The primer sequences used in this study were as follows:

5′-AGAAGGCTGGGGCTCATTTG-3' (GAPDH, forward),
5′-AGGGGCCATCCACAGTCTTC-3' (GAPDH, reverse),
5′- CCATCCAGTTGGGAAGCCAT -3' (TIMP3, forward),
5′- AGCTTCCTTGATTGGGAGGC -3' (TIMP3, reverse),
5′-TCACCGGGTGTAAATCAGCTTG-3' (cel-miR-39),
5′-CTCGCTTCGGCAGCACA-3' (U6, forward),
5′-AACGCTTCACGAATTTGCGT-3' (U6, reverse),
5′-UGAGAACUGAAUUCCAUGGGUU-3' (has-miR-146a).

2.7. Luciferase Reporter Assay. To investigate the regulatory interaction between miR-146a and TIMP3, wild-type and mutant 3′-untranslated region (3′ UTR) fragments of the TIMP3 gene were amplified and cloned into luciferase reporter vectors. HEK293T cells were cotransfected with these constructs, along with miR-146a mimics, miR-146a inhibitors, or their respective negative controls (NCs), using Lipofectamine 3000 (Invitrogen). Firefly luciferase (FL) and Renilla luciferase (RL) activities were measured 48 h post-transfection using a dual-luciferase reporter assay system (Promega, Madison, USA) and a chemiluminescence analyzer (Biosino, Beijing, China). Relative luciferase activity was calculated by normalizing FL signals to RL signals.

2.8. Cell Transfection. HCT116 cells were transfected with miR-146a mimics, inhibitors, or NCs (GenePharma) at a concentration of 100 pmol using Lipofectamine 3000 (Invitrogen) and Opti-MEM (Gibco, USA). After 24 or 48 h, transfected cells were harvested for RNA extraction. For exosome isolation, HCT116 cells were cultured in an RPMI-1640 medium supplemented with exosome-free FBS (C38010050, VivaCell, Shanghai, China). Lentiviral vectors expressing miR-146a, miR-146a inhibitors, or short hairpin RNA (shRNA) targeting TIMP3 (TIMP3-shRNA) were constructed and produced by GeneChem Inc. Transfection efficiency was confirmed using a blank pcDNA3.1 vector as a control.

2.9. Western Blot Analysis. Protein expression levels were assessed by western blotting. Briefly, total protein was extracted, separated by SDS–PAGE, and transferred to PVDF membranes. Membranes were probed with primary antibodies against TSG101 (ab125011, Abcam, 1:1000), CD63 (ab217345, Abcam, 1:1000), Alix (ab186429, Abcam, 1:1000), and TIMP3 (PA5-80131, Cell Signaling Technology, 1:1000). β-actin served as the loading control. After incubation with horseradish peroxidase (HRP)-conjugated secondary antibodies (A32731, Cell Signaling Technology, 1:5000), protein bands were visualized using Super chemiluminescent reagent (HaiGene, Harbin, China) and imaged on a Bio-Rad ChemiDoc XRS system (Bio-Rad, CA, USA).

2.10. Functional Assays

2.10.1. Proliferation Assay. HUVEC proliferation was evaluated using the EdU assay (RiboBio Inc.). Cells were pretreated with exosomes or transfected with miR-146a mimics/inhibitors, followed by incubation with 50 μM EdU for 6 h. Cells were fixed, permeabilized, and stained according to the manufacturer's protocol.

2.10.2. Migration Assay. Cell migration was assessed using wound-healing and transwell assays. For the wound-healing assay, HUVECs were scratched, and wound closure was measured at 0 and 24 h. For the transwell assay, 1×10^5 HUVECs were seeded in a serum-free medium in the upper chamber of transwell inserts (8-μm pore size; Corning, 3422), with 10% FBS medium in the lower chamber. After 6 h, migrated cells were stained with hematoxylin and counted under a light microscope.

2.10.3. Tube Formation Assay. HUVECs were seeded on Matrigel (BD Biosciences)-coated 24-well plates at a density of 1×10^4 cells/well. Tube formation was assessed after 3 h using an optical microscope, and the number of tubes was quantified.

2.11. Immunohistochemistry (IHC). TIMP3 expression in tissue samples was evaluated by IHC as previously described in Ref. [29]. Briefly, tissue sections were incubated with a primary antibody against TIMP3 (ab39184, Abcam, 1:100) overnight at 4°C, followed by incubation with a secondary antibody (ZSGB-BIO, Beijing, China) for 20 min. Staining was visualized using a DAB substrate kit.

2.12. In Vivo Experiments. All animal procedures were approved by the Hospital Scientific Affairs Committee on Animal Research and Ethics and conducted in compliance with the National Institutes of Health (NIH) guidelines for animal care and use. Five-week-old female athymic BALB/c-nu/nu mice (Shanghai SLAC Laboratory Animal Co., Ltd) were housed in specific pathogen-free facilities. For the xenograft model, mice were subcutaneously injected with 1×10^7 HCT116 cells transfected with miR-146a inhibitor lentivirus, miR-146a lentivirus, or control lentivirus. Tumor growth was monitored for 4 weeks, after which mice were euthanized by CO_2 inhalation, and tumor weight and volume were recorded.

2.13. Statistical Analysis. Data are presented as mean ± standard deviation (SD) from at least three independent experiments. Statistical analyses were performed using SPSS 18.0 software. Comparisons between two groups were conducted using a two-tailed Student's *t*-test, while Spearman's correlation analysis was used to evaluate the

relationship between TIMP3 expression and miR-146a levels. A p value < 0.05 was considered statistically significant.

3. Results

3.1. Tumor-Secreted miR-146a Is Enriched in Exosomes of CRC Patients. Given the critical role of angiogenesis in tumor invasion and metastasis, we first explored the differential expression of miRNAs in exosomes derived from CRC patients. RNA sequencing (RNA-seq) was performed on serum exosomal samples from five metastatic CRC (mCRC) patients and five nonmetastatic CRC (non-mCRC) patients (Figure S2). miRNAs with a fold change > 1.5 and $p < 0.05$ were considered differentially expressed. Among these, miR-146a emerged as a key candidate due to its well-documented roles as a proto-oncogene in promoting tumorigenesis and angiogenesis across various cancers [30–32].

To validate the significance of exosomal miR-146a in CRC, serum exosomes were isolated from healthy controls and CRC patients (with or without metastasis) using differential ultracentrifugation. TEM confirmed the characteristic cup-shaped morphology of exosomes (Figure 1(a)), while NTA revealed an average diameter of approximately 120 nm (Figure 1(b)). Western blot analysis confirmed the presence of exosomal markers, including TSG101, Alix, and CD63 (Figure 1(c)). Notably, miR-146a levels were significantly elevated in circulating exosomes from CRC patients compared to healthy controls, with even higher expression observed in metastatic cases (Figure 1(d)).

Further analysis of 16 paired CRC tissues and adjacent normal mucosa revealed upregulation of miR-146a in tumor tissues (Figure 1(e)). Similarly, miR-146a levels were markedly higher in CRC cell lines (HCT116, SW480, SNU-C1, and Lovo) and their secreted exosomes compared to the normal colorectal epithelial cell line NCM460 (Figures 1(f), 1(g)). Postoperative analysis of serum exosomal miR-146a in CRC patients showed a significant reduction in 94% (15/16) of cases following tumor resection (Figure 1(h)). A positive correlation was also observed between miR-146a levels in tumor tissues and circulating exosomes (Figure 1(i)), suggesting that tumor-derived miR-146a contributes to its elevated expression in serum exosomes.

3.2. MiR-146a Enhances the Biological Functions of HUVECs in Vitro. To investigate the functional role of miR-146a in angiogenesis, HUVECs were transfected with miR-146a mimics, inhibitors, or their respective NCs. Overexpression of miR-146a significantly enhanced HUVEC migration (wound-healing assay; Figures 2(a), 2(b)), proliferation (EdU assay; Figures 2(c), 2(d)), invasion (transwell migration assay; Figures 2(e), 2(f)), and tube formation (Figures 2(g), 2(h)). Conversely, miR-146a inhibition suppressed these proangiogenic effects, underscoring its pivotal role in EC function.

3.3. TIMP3 Is a Direct Target of miR-146a in HUVECs. Bioinformatic analysis identified TIMP3 as a potential target of miR-146a. TIMP3, a known tumor suppressor, inhibits angiogenesis and is frequently downregulated in various cancers [33–35]. Luciferase reporter assays confirmed that miR-146a directly binds to the 3′-untranslated region (3′ UTR) of TIMP3 (Figures 3(a), 3(b)). MiR-146a mimics significantly reduced luciferase activity, while inhibitors had the opposite effect (Figure 3(c)). Mutations in the miR-146a binding site abolished these effects, confirming the specificity of the interaction. qRT-PCR and western blot analysis further demonstrated that miR-146a overexpression suppressed TIMP3 mRNA and protein levels in HUVECs, whereas miR-146a inhibition restored TIMP3 expression (Figures 3(d), 3(e), 3(f)). These findings establish TIMP3 as a direct downstream target of miR-146a. To determine whether TIMP3 mediates miR-146a-induced angiogenesis, HUVECs were cotreated with miR-146a inhibitors and TIMP3-shRNA. TIMP3 knockdown reversed the anti-angiogenic effects of miR-146a inhibition, restoring HUVEC proliferation, migration, and tube formation (Supplementary Figures 1B–I). These results suggest that miR-146a promotes angiogenesis by silencing TIMP3 in HUVECs.

3.4. TIMP3 Is Downregulated in CRC Tissues. The clinicopathological features of the 16 CRC patients are shown in Table S1. Analysis of TIMP3 expression in CRC tissues revealed significantly lower mRNA and protein levels in tumor samples compared to adjacent normal tissues (Figures 4(a), 4(b), 4(c)). Immunohistochemical staining further corroborated these findings (Figure 4(d)). A negative correlation was observed between TIMP3 and miR-146a expression in CRC tissues (Figure 4(e)), supporting the hypothesis that TIMP3 acts as a tumor suppressor in CRC.

3.5. CRC-Derived Exosomal miR-146a Promotes Angiogenesis by Silencing TIMP3 in HUVECs. Exosomes are known to mediate intercellular communication by transferring miRNAs between cells [36–38]. To investigate whether CRC-derived exosomes deliver miR-146a to HUVECs, exosomes were isolated from HCT116 cell supernatants and characterized by TEM (Figure 5(a)) and western blotting (Figure 5(b)). HCT116 cells were transfected with miR-146a inhibitors to generate miR-146a-depleted exosomes (Figure 5(c)). Confocal microscopy confirmed the uptake of PKH67-labeled exosomes by HUVECs (Figure 5(d)).

HUVECs treated with miR-146a-depleted exosomes exhibited reduced miR-146a levels and restored TIMP3 expression, whereas control exosomes suppressed TIMP3 (Figures 5(e), 5(f), 5(g)). Functional assays demonstrated that HCT116-derived exosomes enhanced HUVEC migration, proliferation, and tube formation, effects that were attenuated by miR-146a knockdown (Figures 6(a), 6(b), 6(c), 6(d), 6(e), 6(f), 6(g), 6(h)). These findings indicate that CRC-secreted exosomal miR-146a promotes angiogenesis by targeting TIMP3 in HUVECs.

3.6. Exosomal miR-146a Regulates Tumor Growth and Angiogenesis in Vivo. To evaluate the role of miR-146a in tumor progression, a xenograft mouse model was established by subcutaneously injecting HCT116 cells transfected with

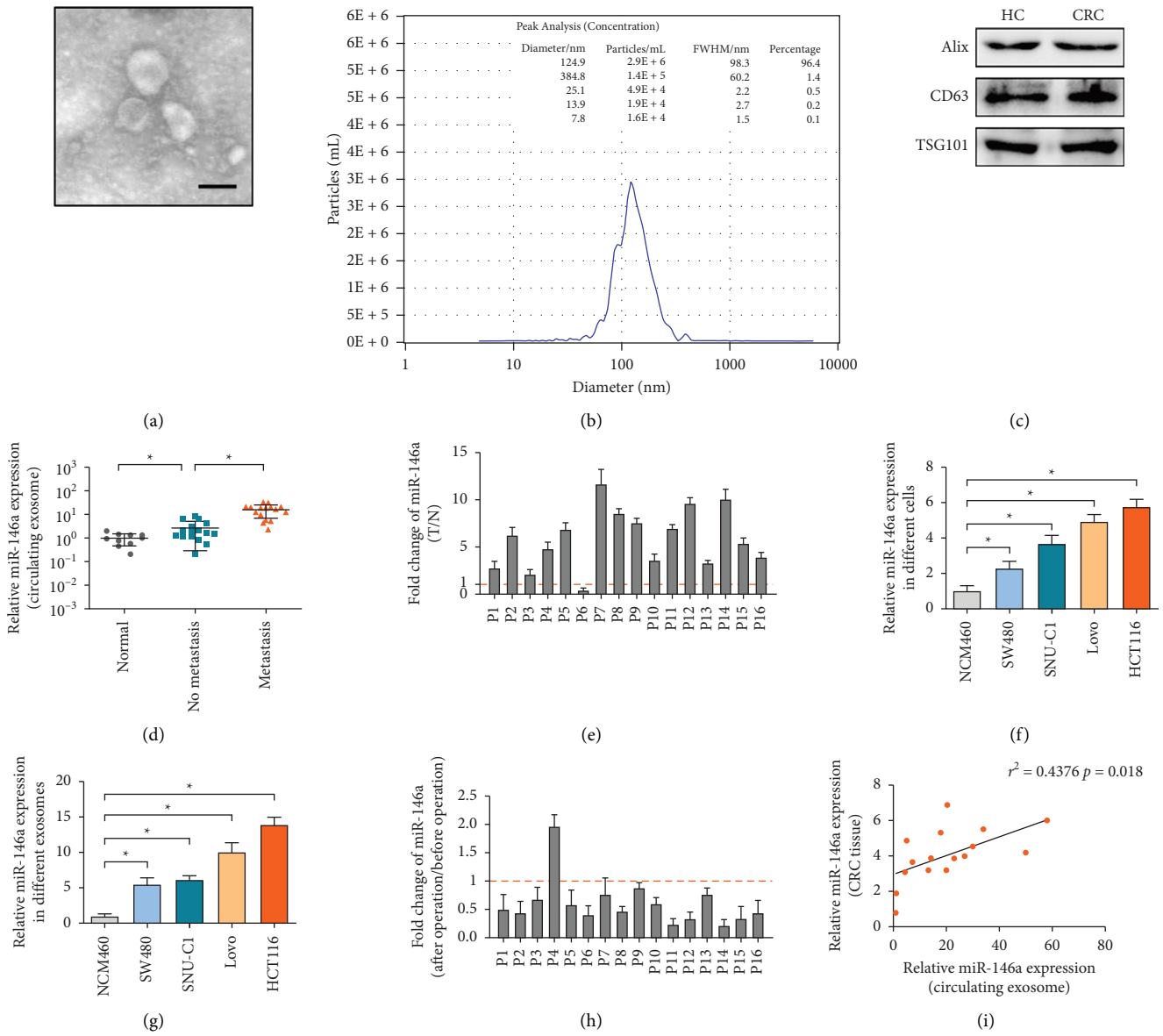

Figure 1: Serum exosomal miR-146a correlates with CRC. (a) Serum exosomes from CRC patients were detected via electron microscopy. Scale bar, 100 nm. (b) NTA of purified exosomes. (c) Western blot analysis for Alix, CD63, and TSG101. (d) miR-146a expression in serum exosomes from healthy controls or CRC patients. (e) RT-PCR analysis of miR-146a expression in 16 paired fresh CRC tissues and matched adjacent normal mucosa samples. (f) miR-146a expression in four CRC cell lines (HCT116, SW480, SNU-C1, and Lovo) and a human colorectal epithelial cell line (NCM460). (g) qRT-PCR analysis of the levels of miR-146a in exosomes from the supernatants of different cell lines. (h) Fold change in miR-146a in serum exosomes from 16 patients after surgery. miR-146a expression at the postoperative stage was normalized to 1. (i) Spearman's correlation analysis between miR-146a expression in CRC tissues and miR-146a expression in circulating exosomes. Pearson's correlation coefficient (r) and the p value are shown, $n = 16$. The p value was derived from Spearman's test. Each experiment was performed in triplicate. Data are presented as mean ± SD. $^*p < 0.05$.

miR-146a-positive, miR-146a-inhibited, or control lentiviruses (Figure 7(a)). Tumor volume and weight were significantly reduced in the miR-146a-negative group compared to the miR-146a-positive group (Figures 7(b), 7(c), 7(d)).

Analysis of tumor tissues revealed higher miR-146a and lower TIMP3 levels in the miR-146a-positive group, with the opposite trend observed in the miR-146a-negative group (Figures 7(e), 7(f)). Serum exosomal miR-146a levels were also elevated in the miR-146a-positive group (Figure 7(g)). Immunohistochemical staining for CD31, a marker of angiogenesis, showed reduced vascular density in tumors from the miR-146a-negative group (Figure 7(h)). These results demonstrate that CRC-derived exosomal miR-146a promotes tumor growth and angiogenesis by down-regulating TIMP3 in vivo.

4. Discussion

Exosomes have emerged as pivotal players in tumorigenesis and intercellular communication, sparking significant

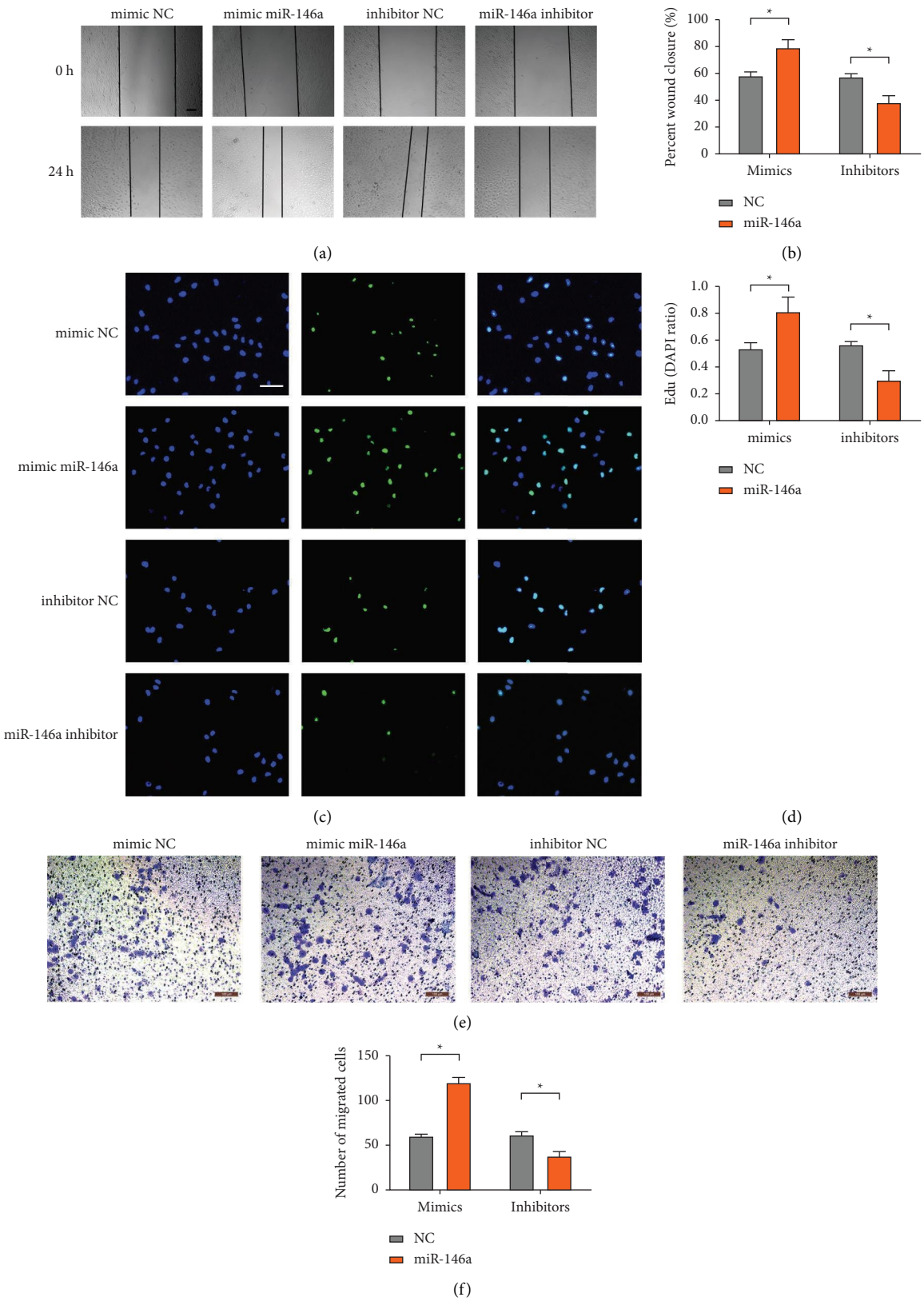

Figure 2: Continued.

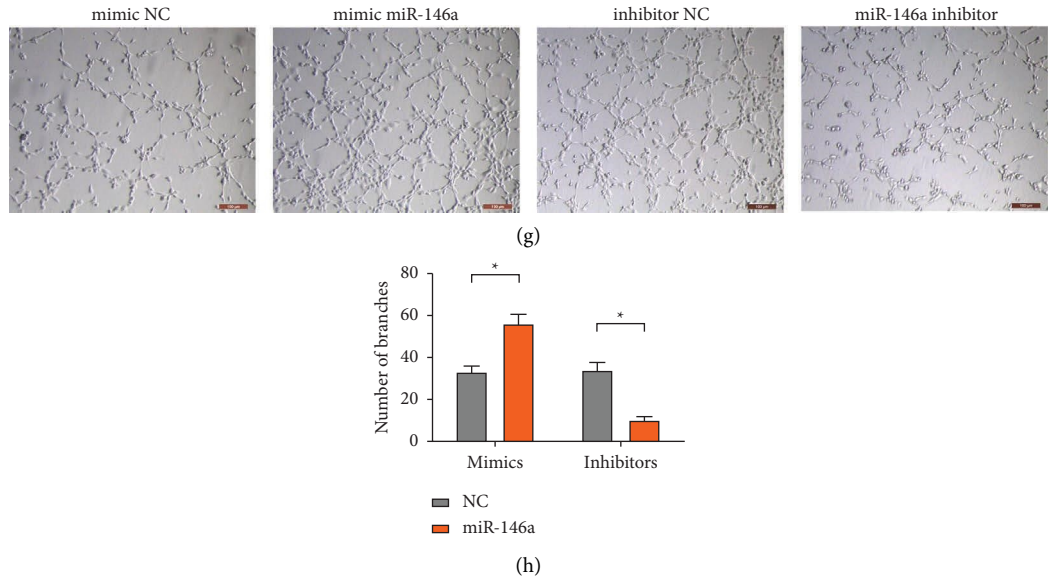

Figure 2: Validation that miR-146a directly promotes the biological function of HUVECs. (a) Wound-healing assay showed that miR-146a promotes HUVEC migration. Scale bar, 100 μm. (b) Quantitative analysis of (a). (c) EdU assay demonstrated that miR-146a enhanced the proliferation of HUVEC. Scale bar, 100 μm. (d) Quantitative analysis of (c). (e) Validation of miR-146a-mediated cell migration via transwell assay. (f) Quantitative analysis of (e). (g) MiR-146a increased the capability of tube formation in HUVECs. (h) Quantitative analysis of (g). All experiments were performed in triplicate. Data are presented as mean ± SD. $^{*}p < 0.05$.

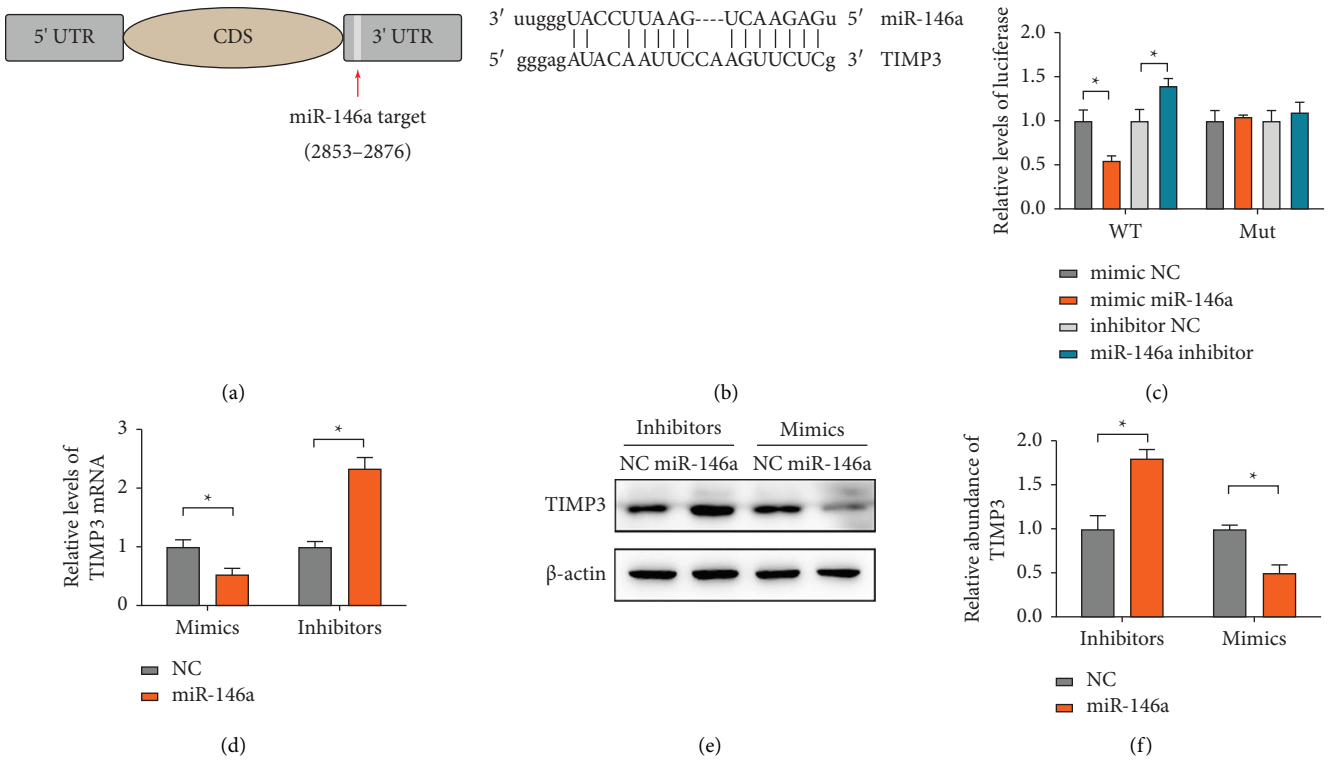

Figure 3: Identification of TIMP3 as a direct target of miR-146a. (a) and (b) Predicted miR-146a binding sites in the 3′ UTR of TIMP3 mRNA. (c) Relative luciferase activity of TIMP3 in HUVECs following transfection with mimic NC, miR-146a mimic, inhibitor NC, or miR-146a inhibitor. (d) qRT-PCR analysis of TIMP3 mRNA in the same treatment groups. (e) Western blot analysis of TIMP3 protein in HUVECs treated with the indicated groups (mimic NC ⟶ mimic miR-146a ⟶ inhibitor NC ⟶ miR-146a inhibitor). (f) Quantification of TIMP3 protein levels from (E). Data are presented as mean ± SD. $^{*}p < 0.05$.

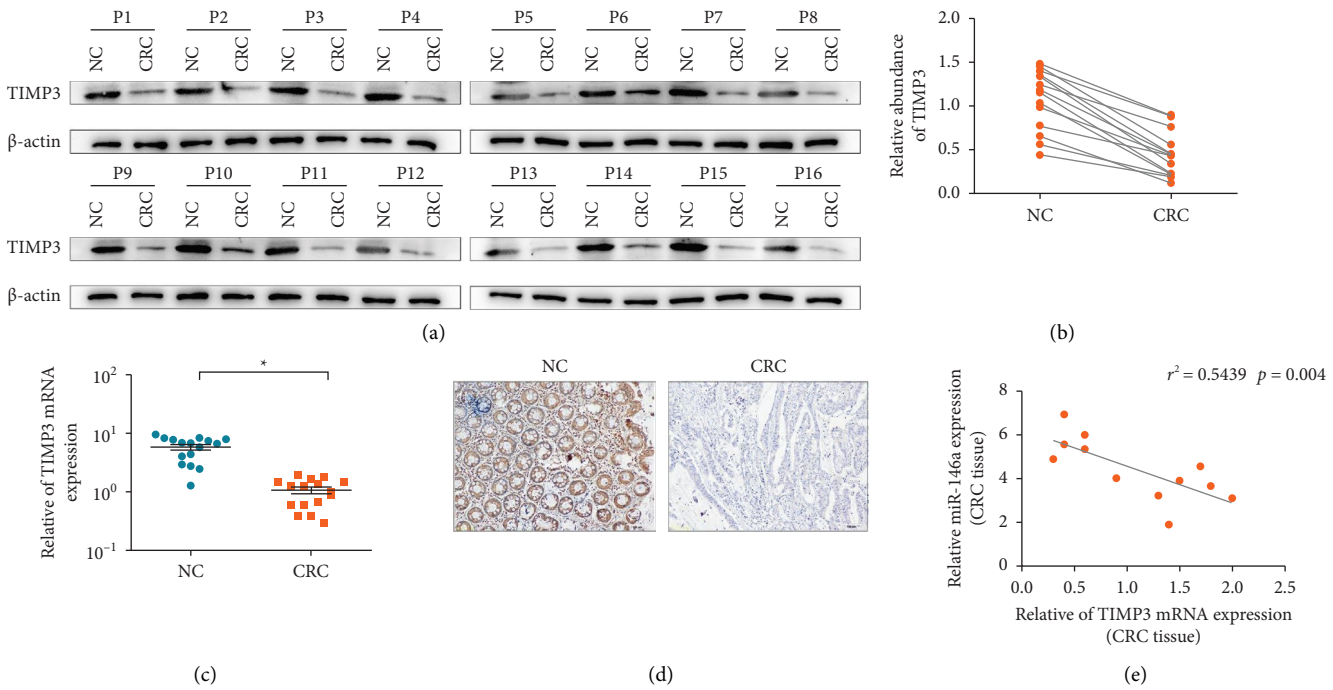

FIGURE 4: TIMP3 expression is decreased in CRC. (a) and (b) Western blot analysis of TIMP3 expression in CRC tumor tissues and paired adjacent noncancerous tissues ($n = 16$). (c) TIMP3 mRNA levels were analyzed in CRC tumor tissues and paired with adjacent noncancerous tissues ($n = 16$). (d) Immunohistochemistry analysis of TIMP3 expression in different groups ($n = 16$). Scale bar, 100 μm. (e) Spearman's correlation analysis showed that miR-146a was negatively correlated with TIMP3 in CRC tumor tissue ($n = 16$). $^*p < 0.05$.

interest and debate in recent years [39]. These extracellular vesicles, secreted by various cell types, serve as carriers for a diverse array of biomolecules, including proteins, lipids, and nucleic acids, facilitating cell-to-cell communication [40]. Their stability in the bloodstream, conferred by a protective lipid bilayer, shields their cargo from enzymatic degradation, enabling them to exert systemic effects. Exosomes are increasingly recognized for their roles in tumor progression, including proliferation, metastasis, and angiogenesis, largely through the regulation of oncogenes and tumor suppressor genes [41–43]. Among their cargo, miRNAs are particularly noteworthy as they can be transported to both nearby and distant recipient cells, where they modulate gene expression and cellular function. Recent studies have highlighted the involvement of exosomes in tumor angiogenesis, a critical process for tumor growth and metastasis. For instance, You et al. [44] demonstrated that gastric cancer-derived exosomes promote vascular growth although the precise molecular mechanisms underlying this phenomenon remain poorly understood and warrant further investigation.

miRNAs, small noncoding RNAs typically 19–25 nucleotides in length, are key regulators of gene expression and play essential roles in numerous biological processes [45]. Dysregulation of miRNAs has been implicated in the promotion of angiogenesis across various cancer types [46]. Among these, miR-146a has garnered attention for its oncogenic properties. It is upregulated in breast cancer and bladder cancer and has been proposed as a potential biomarker for oral cancer. In CRC, miR-146a has been shown to enhance stem-like properties and tumorigenicity. While miR-146a is known to regulate angiogenesis through complex molecular networks, its specific mechanisms in CRC remain to be fully elucidated. Future studies should explore whether previously reported pathways involving miR-146a contribute to its proangiogenic effects in CRC. Although several studies have described miR-146a as a tumor-suppressive miRNAs in certain cancer types, its biological function appears to be highly context-dependent. The divergent roles of miR-146a are likely influenced by the specific cellular environment, target gene repertoire, and tumor type. In CRC, accumulating evidence indicates that miR-146a may act as an oncogenic regulator that promotes tumor growth, stemness, and angiogenesis. Consistent with these findings, our data demonstrate that cancer-derived exosomal miR-146a enhances EC proliferation and tube formation by directly suppressing the antiangiogenic factor TIMP3. These results highlight the dual nature of miR-146a and suggest that its functional outcome depends on the molecular context of the tumor microenvironment.

TIMPs are a family of proteins that regulate extracellular matrix (ECM) remodeling and cell signaling [47]. Among the four mammalian TIMPs, TIMP3 is unique in its ability to bind to the ECM via heparin sulfate proteoglycans and inhibit membrane-associated ADAMs [48]. TIMP3 is a potent tumor suppressor, with high expression levels shown to inhibit the growth of various cancers. It regulates EC apoptosis and directly interacts with vascular endothelial growth factor receptor-2 (VEGFR-2), thereby suppressing angiogenesis and tumor progression [49]. Additionally, TIMP3 acts as a physiological antagonist of matrix metalloproteinases (MMPs), particularly MMP-2 and MMP-9,

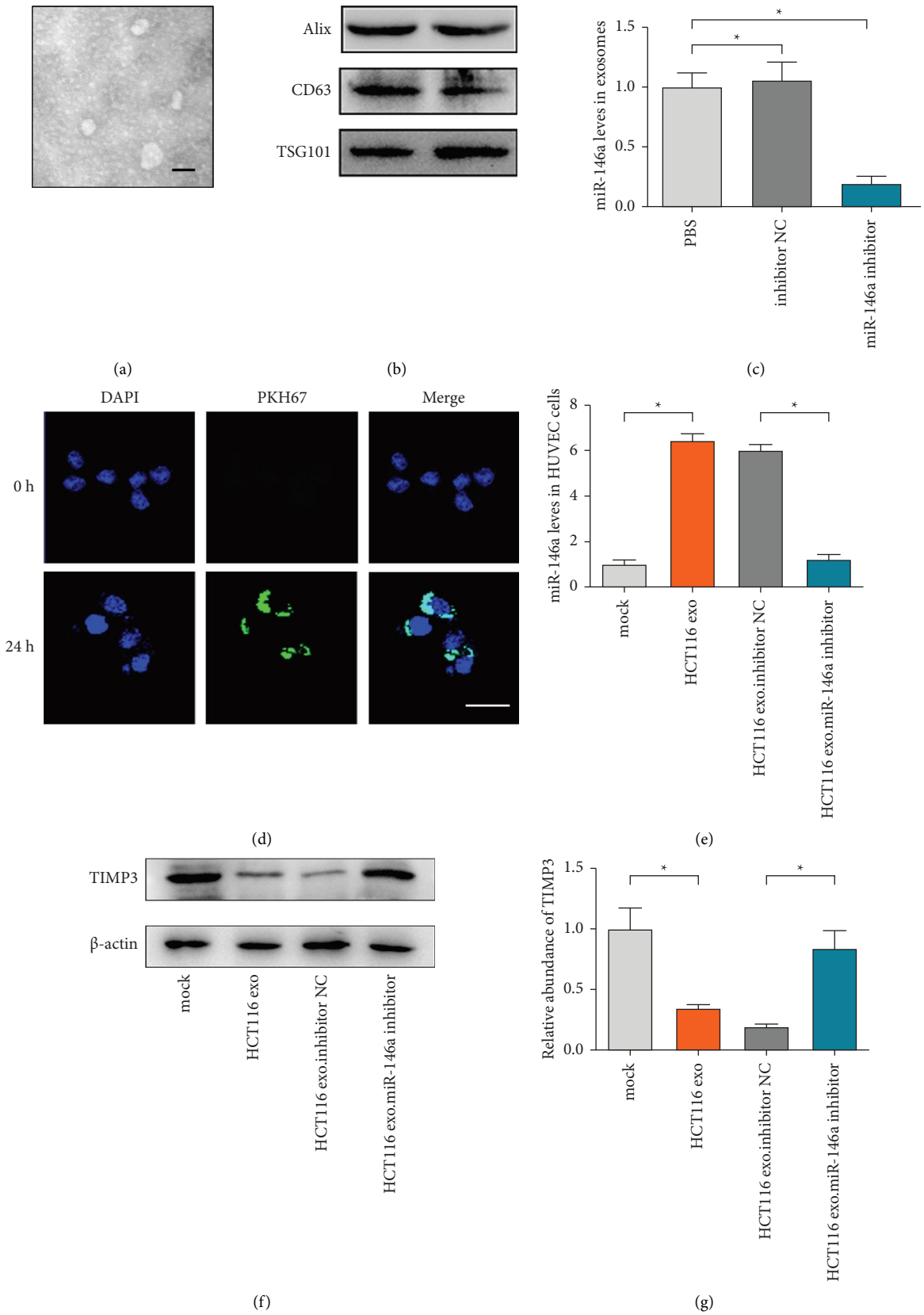

Figure 5: miR-146a can be delivered into HUVECs via exosomes and suppresses TIMP3 expression. (a) Exosomes released by HCT116 cells were detected via electron microscopy. Scale bars, 100 nm. (b) Western blot analysis for TSG101, CD63, and Alix. (c) qRT-PCR analysis of miR-146a levels in exosomes in different treatment groups. (d) Confocal microscopic image of fluorescent labeled HCT116 exosomes after uptake by HUVECs. Scale bar, 50 μm. (e) MiR-146a expression in HUVECs cocultured with different exosomes via qRT-PCR. (f) and (g) Western blot analysis of TIMP3 expression in HUVECs following treatment with different exosomes. All experiments were performed in triplicate. Data are presented as mean ± SD. $^{*}p < 0.05$.

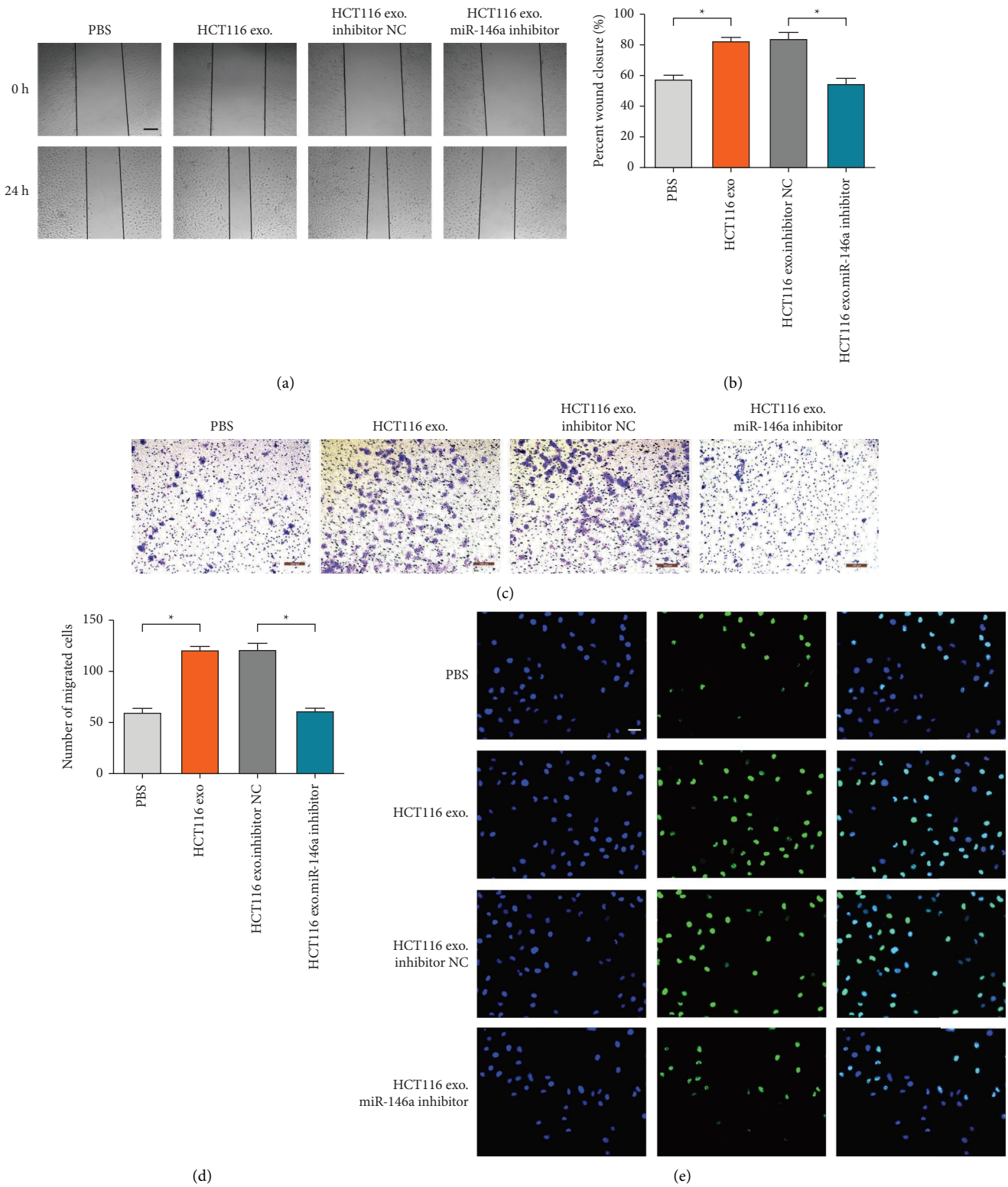

Figure 6: Continued.

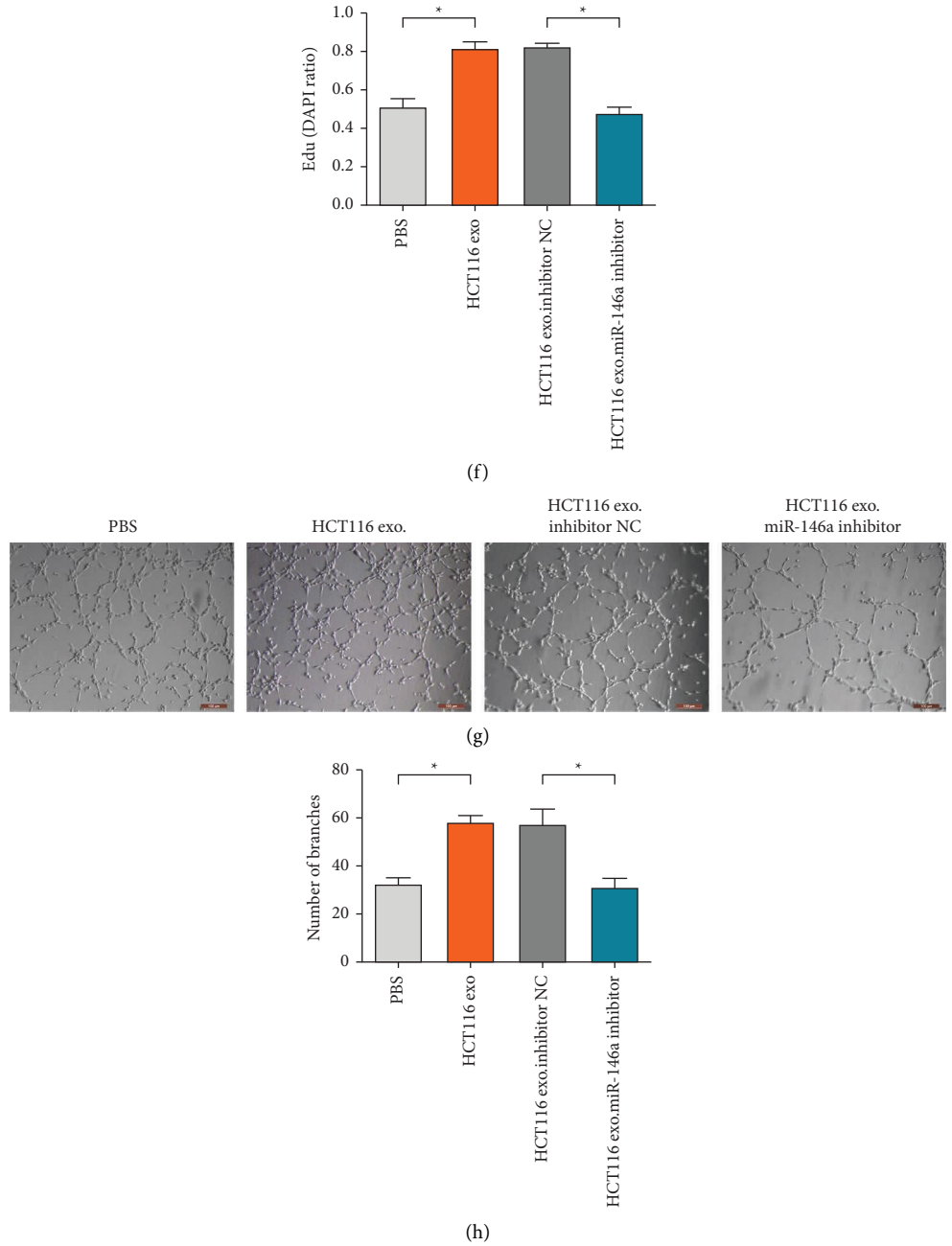

Figure 6: HCT116 exosome-delivered miR-146a promotes angiogenesis. (a) Wound-healing assay results showed that exosomal miR-146a from HCT116 promoted HUVEC migration. Scale bar, 100 μm. (b) Quantitative analysis of (a). (c) Transwell assay results following treatment with PBS or different exosomes. (d) Quantitative analysis of (c). (e) EdU assays showed that HCT116 exosomes promoted HUVEC proliferation. Scale bar, 100 μm. (f) Quantification of (e). (g) Co-incubation with HCT116 exosomes enhanced the capability of tube formation in HUVECs. (h) Quantification of (g). All experiments were performed in triplicate. Data are presented as mean ± SD. $^{*}p < 0.05$ relative to the control.

which are crucial for ECM degradation and EC migration [50]. In this study, we observed significant downregulation of TIMP3 in CRC tissues compared to adjacent normal tissues, suggesting that TIMP3 loss may be a critical event in CRC pathogenesis. We further demonstrated that TIMP3 is a direct functional target of miR-146a in HUVECs, providing mechanistic insight into how CRC-derived exosomal miR-146a promotes angiogenesis by suppressing TIMP3 expression.

The differential expression of miRNAs in the circulatory system of cancer patients has become a focal point in the search for non-invasive biomarkers [51]. Advances in detection technologies have positioned exosomal miRNAs as promising candidates for diagnostic and therapeutic applications. Exosomes serve as a major conduit for the secretion of bioactive molecules by cancer cells, facilitating the delivery of oncogenic miRNAs to establish a protumorigenic microenvironment, including angiogenesis. Detecting

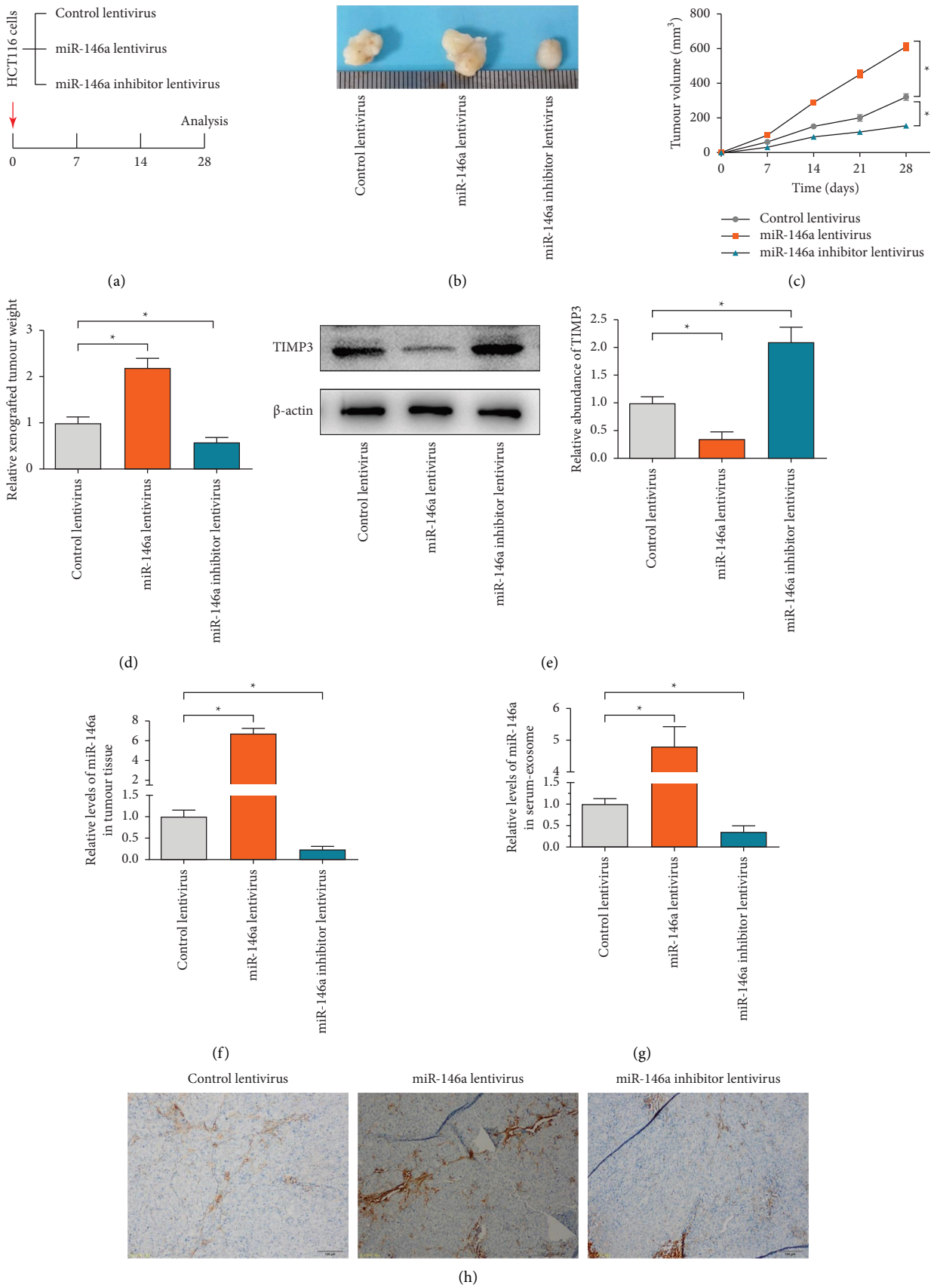
HCT116 cells
Control lentivirus
miR-146a lentivirus
miR-146a inhibitor lentivirus
Analysis
0
7
14
28
(a)
Control lentivirus
miR-146a lentivirus
miR-146a inhibitor lentivirus
(b)
Tumour volume (mm3)
Time (days)
Control lentivirus
miR-146a lentivirus
miR-146a inhibitor lentivirus
(c)
Relative xenografted tumour weight
(d)
TIMP3
β-actin
(e)
Relative abundance of TIMP3
(f)
Relative levels of miR-146a in tumour tissue
(g)
Relative levels of miR-146a in serum-exosome
Control lentivirus
miR-146a lentivirus
miR-146a inhibitor lentivirus
(h)

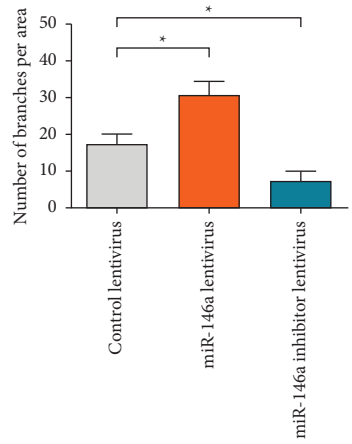

(i)

Figure 7: Pro-angiogenic effect of miR-146a in vivo. (a) Flowchart describing the in vivo experimental design. After transfection with miR-146a inhibitor lentivirus, miR-146a lentivirus, and control group lentivirus, HCT116 cells were injected into mouse groin to establish tumor transplantation model. After 4 weeks, the mice were sacrificed, and the tumor tissues were harvested. (b) Representative tumors harvested from each experimental group are shown ($n = 5$ mice per group). The full quantitative analysis of tumor volume and weight for all mice is presented in panels (c) and (d). (e) The protein levels of TIMP3 in tumors. (f) qRT-PCR analysis of miR-146a in implanted tumors ($n = 5$). (g) MiR-146a expression in serum exosomes of mice in different treatment groups ($n = 5$). (h) Immunohistochemistry analysis of CD31 expression in different paraffin-embedded tumor tissues of mice ($n = 5$) (CD31 is widely used to demonstrate the existence of endothelial tissue and to assess tumor angiogenesis). Scale bar, 100 μm. (i) Quantification of (h). Results are presented as mean ± SD. $^*p < 0.05$. All experiments were carried out in triplicate.

oncogenic miRNAs in exosomes or inhibiting their secretion could provide novel insights into CRC biology, including tumor proliferation, angiogenesis, and invasion. In this study, we found that serum exosomal miR-146a levels were significantly elevated in CRC patients compared to healthy controls. Moreover, miR-146a was highly expressed in CRC tissues relative to adjacent normal mucosa, and its levels in serum exosomes decreased following tumor resection. In vivo experiments further confirmed elevated miR-146a levels in both tumor tissues and circulating exosomes in CRC-bearing mice. These findings suggest that combining miR-146a with other protein biomarkers could enhance the specificity of disease characterization at the individual level, paving the way for personalized antiangiogenic therapies in CRC.

5. Conclusion

In summary, this study demonstrates that elevated levels of circulating exosomal miR-146a drive angiogenesis in CRC by directly targeting and suppressing TIMP3 expression. Our findings highlight the potential of targeting exosomal miR-146a as a novel therapeutic strategy to inhibit angiogenesis in CRC. Specifically, interventions aimed at blocking the release of miR-146a or neutralizing exosomes carrying overexpressed miR-146a could offer promising avenues for antiangiogenic therapy. These insights not only deepen our understanding of the molecular mechanisms underlying CRC progression but also provide a foundation for developing targeted treatments to improve patient outcomes.

Nomenclature

CRC	Colorectal cancer
ECM	Extracellular matrix
ECs	Endothelial cells
FBS	Fetal bovine serum
HUVECs	Human umbilical vein endothelial cells
mCRC	Metastatic colorectal cancer
miRNA	Micro-RNA
NC	Negative control
PBS	Phosphate-buffered saline
PCR	Polymerase chain reaction
RNA-seq	RNA sequencing
shRNA	Short hairpin RNA
TEM	Transmission electron microscopy
TIMP3	Tissue inhibitors of metalloproteinase 3
TIMP3-shRNA	Short hairpin RNA targeting TIMP3.

Data Availability Statement

The data in the current study are available from the corresponding authors upon reasonable request.

Ethics Statement

This study was approved by the Ethics Committee of Peking University Shenzhen Hospital (Shenzhen, China, ID: 2020-332). Written informed consent was obtained from all patients and healthy donors. Animal assays were approved by the Hospital Scientific Affairs Committee on Animal Research and Ethics.

Consent

Please see the Ethics Statement.

Conflicts of Interest

The authors declare no conflicts of interest.

Author Contributions

Zhengqiang Wei: conceptualization. **He Liu:** formal analysis, funding acquisition, validation, visualization, and writing–original draft. **Tianyi Xia, Xiaolong Liang, Song Xiang, Zhenzhou Chen, and Yang Pan:** data curation. **He Liu and Zhengqiang Wei**: writing–review and editing.

Funding

This work was supported by the National Natural Science Foundation of China (Grant Number 82403569).

Supporting Information

Additional supporting information can be found online in the Supporting Information section.

Supporting Information 1. Figure S1. TIMP3 is a functional target of miR-146a in HUVECs. **(A)** qRT-PCR analysis of the relative miR-146a content in HUVECs after treatment with miR-146a mimic or inhibitor. **(B)** TIMP3 mRNA levels were analyzed in the different groups via qRT-PCR. **(C)** Immunoblotting was used to detect the expression of TIMP3 in HUVECs treated with TIMP3-shRNA or control group shRNA. **(D)** EdU assays showed that TIMP3 could inhibit the proliferation of HUVECs. Scale bar, 100 μm. **(E)** Quantitative analysis of (D). **(F)** Transwell assay showed that TIMP3 could inhibit the migration of HUVECs. Scale bar, 100 μm. **(G)** Quantitative analysis of (F). **(H)** TIMP3 inhibited the tube-forming capability of HUVECs. Scale bar, 100 μm. **(I)** Quantitative analysis of **(H)**. All of the experiments were performed in triplicate, and data were presented as mean ± SD. $^{*}p < 0.05$.

Supporting Information 2. Figure S2. Differential expression of exosomal miRNAs in CRC patients with or without metastasis. Heatmap showing the expression profiles of differentially expressed serum exosomal miRNAs from metastatic CRC (mCRC) and nonmetastatic CRC (non-mCRC) patients. Red indicates high expression, and blue indicates low expression. miR-146a-5p (highlighted with a red box) was among the significantly upregulated miRNAs in metastatic CRC patients, and the Venn diagram shows the overlap and unique distribution of exosomal miRNAs between the two groups. A total of 922 miRNAs were commonly expressed, while 152 miRNAs were unique to the non-mCRC group and 152 miRNAs were unique to the mCRC group.

Supporting Information 3. Supplementary Table 1. Clinicopathologic features of 16 CRC patients.

References

[1] E. Morgan, M. Arnold, A. Gini, et al., "Global Burden of Colorectal Cancer in 2020 and 2040: Incidence and Mortality Estimates from GLOBOCAN," *Gut* 72, no. 2 (2023): 338–344, https://doi.org/10.1136/gutjnl-2022-327736.

[2] T. B. Kratzer, A. Jemal, K. D. Miller, et al., "Cancer Statistics for A Merican I Ndian and A Laska N Ative Individuals, 2022: including Increasing Disparities in Early Onset Colorectal Cancer," *CA: A Cancer Journal for Clinicians* 73, no. 2 (2023): 120–146, https://doi.org/10.3322/caac.21757.

[3] R. L. Siegel, N. S. Wagle, A. Cercek, R. A. Smith, and A. Jemal, "Colorectal Cancer Statistics, 2023," *CA: A Cancer Journal for Clinicians* 73, no. 3 (2023): 233–254, https://doi.org/10.3322/caac.21772.

[4] Y. Guo, Y. Guo, C. Chen, et al., "Circ3823 Contributes to Growth, Metastasis and Angiogenesis of Colorectal Cancer: Involvement of miR-30c-5p/TCF7 Axis," *Molecular Cancer* 20, no. 1 (2021): 93, https://doi.org/10.1186/s12943-021-01372-0.

[5] B. T. Oggesen, M. L. S. Hamberg, and J. Rosenberg, "Practical Management Algorithms for Late Complications After Colorectal and Anal Cancer—Basic Treatment of Late Complications," *Medicine Advances* 1, no. 3 (2023): 260–269, https://doi.org/10.1002/med4.32.

[6] B. Thing Oggesen and J. Rosenberg, "Psychosocial Challenges After Treatment for Colorectal and Anal Cancer: a Descriptive Study," *Medicine Advances* 3, no. 3 (2025): 197–201, https://doi.org/10.1002/med4.70020.

[7] Z. Wu, C. Xiao, J. Long, W. Huang, F. You, and X. Li, "Mitochondrial Dynamics and Colorectal Cancer Biology: Mechanisms and Potential Targets," *Cell Communication and Signaling* 22, no. 1 (2024): 91, https://doi.org/10.1186/s12964-024-01490-4.

[8] F. Di Nicolantonio, P. P. Vitiello, S. Marsoni, et al., "Precision Oncology in Metastatic Colorectal Cancer—From Biology to Medicine," *Nature Reviews Clinical Oncology* 18, no. 8 (2021): 506–525, https://doi.org/10.1038/s41571-021-00495-z.

[9] S. G. Patel, J. J. Karlitz, T. Yen, C. H. Lieu, and C. R. Boland, "The Rising Tide of Early-Onset Colorectal Cancer: a Comprehensive Review of Epidemiology, Clinical Features, Biology, Risk Factors, Prevention, and Early Detection," *The lancet Gastroenterology & hepatology* 7, no. 3 (2022): 262–274, https://doi.org/10.1016/s2468-1253(21)00426-x.

[10] T. Heide, J. Househam, G. D. Cresswell, et al., "The Co-Evolution of the Genome and Epigenome in Colorectal Cancer," *Nature* 611, no. 7937 (2022): 733–743, https://doi.org/10.1038/s41586-022-05202-1.

[11] R. Shang, S. Lee, G. Senavirathne, and E. C. Lai, "microRNAs in Action: Biogenesis, Function and Regulation," *Nature Reviews Genetics* 24, no. 12 (2023): 816–833, https://doi.org/10.1038/s41576-023-00611-y.

[12] K. Das and L. V. M. Rao, "The Role of microRNAs in Inflammation," *International Journal of Molecular Sciences* 23, no. 24 (2022): 15479, https://doi.org/10.3390/ijms232415479.

[13] S. Cai, T. Pataillot-Meakin, A. Shibakawa, et al., "Single-Molecule Amplification-Free Multiplexed Detection of Circulating Microrna Cancer Biomarkers from Serum," *Nature Communications* 12, no. 1 (2021): 3515, https://doi.org/10.1038/s41467-021-23497-y.

[14] G. A. Metcalf, "MicroRNAs: Circulating Biomarkers for the Early Detection of Imperceptible Cancers via Biosensor and machine-learning Advances," *Oncogene* 43, no. 28 (2024): 2135–2142, https://doi.org/10.1038/s41388-024-03076-3.

[15] D. Yadav and R. Malviya, "Novel Nanomaterials as Photo-Activated Cancer Diagnostics and Therapy," *Medicine Advances* 1, no. 3 (2023): 190–209, https://doi.org/10.1002/med4.36.

[16] Y. Tang, S. Zong, H. Zeng, et al., "MicroRNAs and Angiogenesis: a New Era for the Management of Colorectal Cancer," *Cancer Cell International* 21, no. 1 (2021): 221, https://doi.org/10.1186/s12935-021-01920-0.

[17] S. Vimalraj, "A Concise Review of VEGF, PDGF, FGF, Notch, Angiopoietin, and HGF Signalling in Tumor Angiogenesis With a Focus on Alternative Approaches and Future Directions," *International Journal of Biological Macromolecules* 221 (2022): 1428–1438, https://doi.org/10.1016/j.ijbiomac.2022.09.129.

[18] K. Yang, Q. Zhou, B. Qiao, et al., "Exosome-Derived Noncoding RNAs: Function, Mechanism, and Application in Tumor Angiogenesis," *Molecular Therapy Nucleic Acids* 27 (2022): 983–997, https://doi.org/10.1016/j.omtn.2022.01.009.

[19] Q. Zheng and W. Hou, "Regulation of Angiogenesis by microRNAs in Cancer," *Molecular Medicine Reports* 24, no. 2 (2021): 583, https://doi.org/10.3892/mmr.2021.12222.

[20] J. Liao, W. He, L. Li, et al., "Mitochondria in Brain Diseases: Bridging structural-mechanistic Insights into precision-targeted Therapies," *Cell Biomaterials* 1, no. 2 (2025): 100016, https://doi.org/10.1016/j.celbio.2025.100016.

[21] J. Zang, Z. Ren, H. Wang, et al., "Emerging Nanozyme Strategies for Precision Breast Cancer Treatment," *Advanced Science* (2025): e14085, https://doi.org/10.1002/advs.202514085.

[22] J. B. Foo, Q. H. Looi, C. W. How, et al., "Mesenchymal Stem Cell-Derived Exosomes and MicroRNAs in Cartilage Regeneration: Biogenesis, Efficacy, miRNA Enrichment and Delivery," *Pharmaceuticals* 14, no. 11 (2021): 1093, https://doi.org/10.3390/ph14111093.

[23] J. Li, J. Wang, and Z. Chen, "Emerging Role of Exosomes in Cancer Therapy: Progress and Challenges," *Molecular Cancer* 24, no. 1 (2025): 13, https://doi.org/10.1186/s12943-024-02215-4.

[24] X. Wang, L. Tian, J. Lu, and I. O.-L. Ng, "Exosomes and cancer-Diagnostic and Prognostic Biomarkers and Therapeutic Vehicle," *Oncogenesis* 11, no. 1 (2022): 54, https://doi.org/10.1038/s41389-022-00431-5.

[25] Q. Huang, J. Liao, J. Li, et al., "Curcumin-Loaded Ceria Nanoenzymes for Dual-Action Suppression of Inflammation and Alleviation of Oxidative Damage in the Treatment of Acute Lung Injury," *Chinese Chemical Letters* 36, no. 4 (2025): 109914, https://doi.org/10.1016/j.cclet.2024.109914.

[26] J. Liao, W. He, S. Zhang, et al., "Magnetic Field Driven Ceria Nanosystems for Mitochondria Targeted Therapy of Ischemic Stroke," *Advanced Functional Materials* 35, no. 24 (2025): 2423291, https://doi.org/10.1002/adfm.202423291.

[27] Q.-F. Han, W.-J. Li, K.-S. Hu, et al., "Exosome Biogenesis: Machinery, Regulation, and Therapeutic Implications in Cancer," *Molecular Cancer* 21, no. 1 (2022): 207, https://doi.org/10.1186/s12943-022-01671-0.

[28] G. Guo, Z. Tan, Y. Liu, F. Shi, and J. She, "The Therapeutic Potential of Stem Cell-Derived Exosomes in the Ulcerative Colitis and Colorectal Cancer," *Stem Cell Research & Therapy* 13, no. 1 (2022): 138, https://doi.org/10.1186/s13287-022-02811-5.

[29] H. Liu, Y. Li, J. Li, Y. Liu, and B. Cui, "H3K4me3 and Wdr82 are Associated with Tumor Progression and a Favorable Prognosis in Human Colorectal Cancer," *Oncology Letters* 16, no. 2 (2018): 2125–2134, https://doi.org/10.3892/ol.2018.8902.

[30] J. R. Iacona and C. S. Lutz, "miR-146a-5p: Expression, Regulation, and Functions in Cancer," *Wiley Interdisciplinary Reviews RNA* 10, no. 4 (2019): e1533, https://doi.org/10.1002/wrna.1533.

[31] J. Zhuang, L. Shen, M. Li, et al., "Cancer-Associated Fibroblast–Derived miR-146a-5p Generates a Niche that Promotes Bladder Cancer Stemness and Chemoresistance," *Cancer Research* 83, no. 10 (2023): 1611–1627, https://doi.org/10.1158/0008-5472.can-22-2213.

[32] M. Alimohammadi, D. Amani, I. Adcock, and E. Mortaz, "Dual Role of mir-146a in Non-Small Cell Lung Cancer Progression: Molecular Mechanisms and Clinical Potential," *Cellular Signalling* 136 (2025): 112115, https://doi.org/10.1016/j.cellsig.2025.112115.

[33] M. Mazzoni, K. Todoerti, L. Agnelli, et al., "Transcriptomic Landscape of TIMP3 Oncosuppressor Activity in Thyroid Carcinoma," *Cancer Cell International* 22, no. 1 (2022): 400, https://doi.org/10.1186/s12935-022-02811-8.

[34] N. Bhola, A. K. Jaiswal, and D. Saluja, "An Integrative Bioinformatics Approach to Investigating TIMP3 and Immune Cell Infiltration: Prognostic and Clinicopathological Implications," *International Journal of Molecular Sciences* 26, no. 18 (2025): 8867, https://doi.org/10.3390/ijms26188867.

[35] W.-T. Lee, P.-Y. Wu, Y.-M. Cheng, and Y.-F. Huang, "Tissue Inhibitor of Metalloproteinase 3: Unravelling its Biological Function and Significance in Oncology," *International Journal of Molecular Sciences* 25, no. 6 (2024): 3191, https://doi.org/10.3390/ijms25063191.

[36] Y. Huang, M. Kanada, J. Ye, et al., "Exosome-Mediated Remodeling of the Tumor Microenvironment: From Local to Distant Intercellular Communication," *Cancer Letters* 543 (2022): 215796, https://doi.org/10.1016/j.canlet.2022.215796.

[37] R. Isaac, F. C. G. Reis, W. Ying, and J. M. Olefsky, "Exosomes as Mediators of Intercellular Crosstalk in Metabolism," *Cell Metabolism* 33, no. 9 (2021): 1744–1762, https://doi.org/10.1016/j.cmet.2021.08.006.

[38] L. R. Lizarraga-Valderrama and G. K. Sheridan, "Extracellular Vesicles and Intercellular Communication in the Central Nervous System," *FEBS Letters* 595, no. 10 (2021): 1391–1410, https://doi.org/10.1002/1873-3468.14074.

[39] W. Han, H. Zhang, L. Feng, et al., "The Emerging Role of Exosomes in Communication Between the Periphery and the Central Nervous System," *MedComm* 4, no. 6 (2023): e410, https://doi.org/10.1002/mco2.410.

[40] H. Zhang, J. Xing, Z. Dai, D. Wang, and D. Tang, "Exosomes: the Key of Sophisticated Cell–Cell Communication and Targeted Metastasis in Pancreatic Cancer," *Cell Communication and Signaling* 20, no. 1 (2022): 9, https://doi.org/10.1186/s12964-021-00808-w.

[41] M. D. A. Paskeh, M. Entezari, S. Mirzaei, et al., "Emerging Role of Exosomes in Cancer Progression and Tumor Microenvironment Remodeling," *Journal of Hematology & Oncology* 15, no. 1 (2022): 83, https://doi.org/10.1186/s13045-022-01305-4.

[42] X. Shi, Y. Zhao, H.-Y. Gao, et al., "NFS1, Together with FXN, Protects Cells from Ferroptosis and DNA Damage in Diffuse Large B-cell Lymphoma," *Redox Biology* 87 (2025): 103878, https://doi.org/10.1016/j.redox.2025.103878.

[43] Y. Zhu, Q. Xi, Y. Liu, Y. Zhou, J. Liao, and Q. Wu, "Recent Advances in Exosome-Based Nanodelivery Systems for Parkinson's Disease," *Biomaterials* 325 (2025): 123548, https://doi.org/10.1016/j.biomaterials.2025.123548.

[44] X. You, W. Sun, Y. Wang, et al., "Cervical Cancer-Derived Exosomal miR-663b Promotes Angiogenesis by Inhibiting Vinculin Expression in Vascular Endothelial Cells," *Cancer*

Cell International 21, no. 1 (2021): 684, https://doi.org/10.1186/s12935-021-02379-9.

[45] L.-L. Chen and V. N. Kim, "Small and Long Non-Coding RNAs: past, Present, and Future," *Cell* 187, no. 23 (2024): 6451–6485, https://doi.org/10.1016/j.cell.2024.10.024.

[46] D. C. Stieg, Y. Wang, L.-Z. Liu, and B.-H. Jiang, "ROS and miRNA Dysregulation in Ovarian Cancer Development, Angiogenesis and Therapeutic Resistance," *International Journal of Molecular Sciences* 23, no. 12 (2022): 6702, https://doi.org/10.3390/ijms23126702.

[47] X. Wang and R. A. Khalil, "Matrix Metalloproteinases, Vascular Remodeling, and Vascular Disease," *Advances in Pharmacology* 81 (2018): 241–330, https://doi.org/10.1016/bs.apha.2017.08.002.

[48] V. Arpino, M. Brock, and S. E. Gill, "The Role of TIMPs in Regulation of Extracellular Matrix Proteolysis," *Matrix Biology* 44-46 (2015): 247–254, https://doi.org/10.1016/j.matbio.2015.03.005.

[49] E. Pawluczuk, M. Łukaszewicz-Zając, and B. Mroczko, "The Comprehensive Analysis of Specific Proteins as Novel Biomarkers Involved in the Diagnosis and Progression of Gastric Cancer," *International Journal of Molecular Sciences* 24, no. 10 (2023): 8833, https://doi.org/10.3390/ijms24108833.

[50] J. Hou, K. Mei, D. Wang, et al., "TGM1/3-Mediated Transamidation of Exo70 Promotes Tumor Metastasis Upon LKB1 Inactivation," *Cell Reports* 43, no. 8 (2024): 114604, https://doi.org/10.1016/j.celrep.2024.114604.

[51] A. Ghit and H. E. Deeb, "Cytokines, miRNAs, and Antioxidants as Combined Non-Invasive Biomarkers for Parkinson's disease," *Journal of Molecular Neuroscience* 72, no. 5 (2022): 1133–1140, https://doi.org/10.1007/s12031-022-01984-1.